Novel design and evaluation of a fast response luminescence-based fiber-optic pH and O_2 sensors

J Werner[1], M Belz[3], K-F Klein[2,3], T Sun[1] and K T V Grattan[1]
[1]*School of Science & Technology, City, University of London, London, UK*
[2]*THM, University of Applied Science, 61169 Friedberg, Germany*
[3]*Lytegate GmbH, 61169 Friedberg, Germany*

Dedicated to Professor Bishnu P Pal for his enormous contributions to the advancement of research and education in science and technology through his unique vision and outstanding dedication

Even though many different designs for currently available, fluorescence-based fiber optic sensors for measuring pH and oxygen concentration (O_2) are well known (and often commercially available), they often are limited by their response time and drift. This can cause problems in the important applications of fiber optic sensors of this type, evident for example in physiology and other fields. Research by a number of groups has discussed the various new designs of fiber optical sensors which have been developed: key features of such probes are, for example, tip shape and coating layer thickness. This research reported here has concerned the performance of several new fiber optic-based sensors where fast response has been the priority: achieving response times of < 5 second for pH sensing and < 0.4 second for oxygen (O_2) sensors. The performance of a group of sensors of this type have been analyzed, examining sensor accuracy, mechanical stability and overall long term stability, as well as any cross-sensitivity to any temperature changes which may be experienced.

Keywords: fiber-optics; optical fiber sensors; O_2 measurement; pH sensing; fast response time; luminescence; fluorescence; microsensor; optical sensors; instrumentation; fiber-optic; commercial; biomedical measurements.

1 Introduction

There is a particular interest in detecting key parameters for the clinical analysis of blood [1], for quality control in the food and beverage industries[2], for process control in bioreactors [3, 4] or for seawater pollution analysis [5, 6], where the determination of pH and oxygen concentration (O_2) are particularly important parameters. Further applications are evident across industry, in environmental monitoring and in biomedical research, for example and the field has been the subject of several review papers written in recent years e.g. [7]. The Clark electrode [8] and the pH glass electrode [9] are commonly used in industry for O_2 concentration measurement and the determination of pH value. However, sensors of this type consume the analyte, and this issue can cause problems in some situations. Further, these sensors can experience interference from stray electromagnetic fields in certain industrial situations. Above all, they are fragile (they are made from glass) and often bulky, which require them to be handled very carefully, especially for in-the-field use.

As an alternative to such sensors, fiber optical sensors are becoming more widely used in measurements like these since they do not consume the analyte (e.g. O_2), are reversible and above all, given the small size of the fiber itself, are easy to miniaturize (< 50µm). Further, they can be employed in either the gas or the liquid phase, are inexpensive and if there is electromagnetic interference present, they are unaffected[10]. The market for such optical fiber sensors is thus growing, and especially so for pH and O_2 measurement. Looking at the development since 2000, more of these sensors are now commercially available, designed for a wide range of commercial and industrial applications. Companies such as PreSens Precision Sensing GmbH (www.presens.de), World Precision Instruments Inc.(www.wpiinc.com), Ocean Insight Inc. (www.oceaninsight.com), PyroScience GmbH (www.pyroscience.com), Unisense (www.unisense.com), Ohio Lumex (www.ohiolumex.com) now have a significant presence in the market and research developments reported some years ago in the literature are now coming to fruition in commercially available products. In that way, the users of this type of sensors can access many different system designs: they vary from the large (and thus robust) [11–14] to very small [15–19]. In that way, the wide range of applications to which they can be applied can be addressed, with products at different prices and with different specifications to suit the different applications.

Absorbance, reflectance or luminescence-based techniques are amongst most widely used for pH or O_2 sensing for a number of reasons. Different types of indicator dyes can be used for pH (e.g. SNARF, SNAFL, HPTS and fluorescein) [20] and O_2 concentration (e.g. complexes of Ru(II), Ir(II), Pt(II) and Pd(II)) that offer a luminescence intensity, luminescence decay time or ratiometric (absorbance or luminescence)-based measurements [10, 21]. The detection of luminescence intensity or decay time is a simple and easy to use route to a measurand-sensitive parameter (in comparison to ratiometric measurements, as only one type of indicator dye is needed) and so the detection systems are simpler to design – reducing the number of excitation sources and emission detectors, with concomitant cost benefits. Problems still do arise, unfortunately, due to photobleaching, or if not well designed resulting from stray light and the drift of the electronic components used [21]. Such problems can be reduced or eliminated by better systems design.

Most fiber optic sensors of this type use an indicator dye immobilized in a supporting matrix, which typically is a polymer, attached to the sensor tip [22]. The sensor response time, drift and detection range – the key performance indicators – are influenced by the synergy of the effects on the sensor platform (here the fiber tip), the type of polymer and the indicator dye that have been used [23]. Optimization of the sensor tip design is clearly important as a smaller tip can reduce the response time (although typically will mean a smaller amount of indicator is present at the tip itself, as is the choice of optical fiber chosen which will make a difference to the guidance of the light launched [24, 25]).

Over the years, a number of different luminescence-based O_2 sensors have been reported, with response times to O_2 changes (to 90% of saturation – Δt_{90}) ranging widely, from 3.7 s to 100 s [26–30]. Market surveys carried out shows that the luminescence-based pH sensors typically available have response times (Δt_{90}) from ~20 s to an extreme of 50 minutes in some cases [11–15, 17, 18, 31]. Having shorter response times is important for many applications, and so the aim in the research carried out has been to reduce this parameter, but at the same time maintaining the sensor stability and accuracy. The sensor reported here has been designed around an innovative, specially-formed and chemically-treated fiber tip – in that way permitting the use of thinner fiber tip coatings in the sensor design and improving the sensor performance, giving a faster response time when compared to what has been reported in the literature for a range of different luminescence-based O_2 and pH sensors. Further work in the design process has targeted improving performance by reducing photo-bleaching and stray light effects, as these are performance-limiting in many commercial sensors.

The pH-sensitive coating used is based on an indicator dye (fluorescein-O-methacrylate) immobilised in a hydrogel, which reacts effectively to pH changes in the range of pH 5 to pH 8.5. Thus pH changes are detected by measuring the luminescence intensity. Further, the O_2 sensitive coating frequently used for that sensor employs an indicator dye (PtTFPP), allowing it to cover the physiologically important O_2 (0 % to 20 %) range. In this case, the dye is physically entrapped in a polymer (polystyrene) matrix and O_2 concentration changes are detected using the luminescence decay time changes (this being measured with a commercially available instrument) and having the advantage that changes in luminescent intensity will not, in principle, affect the decay time measurement.

The work reported in this paper discusses the considerable progress made, and thus the O_2 and pH sensors developed which are seen to be very stable over a long period of time, designed to have the short response time needed for use in 'real world' situations. Since the conditions under which such sensors are used are often far from ideal, external effects, such as the influence of temperature and mechanical stability, were investigated in order to be able to correct any cross-sensitivities.

2 Theoretical background: luminescence-based determination of pH and O_2

Luminescence signal measurements (either optical intensity or decay time) are used in this work and so a short theoretical background on the determination of the pH and O_2 concentrations is discussed here.

2.1 Principle of O_2 quenching and common models

The photoluminescence of many luminescent materials, such as the one used for the O_2 sensor in this work, can be affected by various processes known as quenching. The presence of molecular O_2 reduces the luminescence

intensity and the lifetime, due to dynamic collision quenching of O_2 molecules in the excited electronic state S_1 (see Figure 1); no photon emission is seen when returning to the ground state (S_0) – this does not change the molecule and is fully reversible [21, 32].

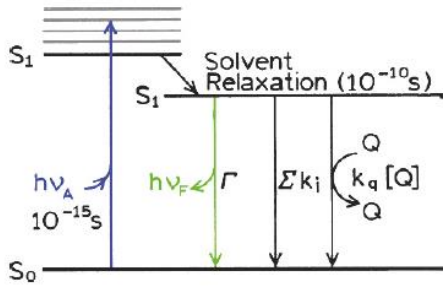

Fig 1. Modified Jablonski Diagram illustrating the process of collision quenching [32].

The Stern-Volmer equation describes this photophysical effect caused by collisional O_2 quenching, as follows:

$$\frac{I_0}{I} = \frac{\tau_0}{\tau} = 1 + K_{SV}[O_2] \quad (1)$$

where τ_0 is the decay time and I_0 the luminescence intensity in absence of O_2. Additionally, τ is the decay time and I the luminescence intensity in presence of O_2 where K_{SV} is the Stern Volmer constant and $[O_2]$ the concentration of O_2 present. However, the Stern-Volmer equation only describes an ideal quenching system, and unfortunately many luminescent indicator dyes show non-linear behaviors. To take this into consideration, an alternative, popular model (the Lehrer quenching model) has been found to be a good way to describe the effect of a quenchable and a non-quenchable site. This approach has been used to calibrate the O_2 sensors [7], as follows:

$$\frac{I_0}{I} = \frac{\tau_0}{\tau} = \left(\frac{f}{1 + K_{SV}[O_2]} + (1 - f)\right)^{-1} \quad (2)$$

where f represents the contribution of the quenchable part and (1 – f) the contribution of the non-quenchable part of a luminescent material to the total luminescence emission.

2.2 Principle of pH measurement based on fluorescence intensity

The activity of hydrogen ions in aqueous solutions can be measured directly using classical electrochemical sensors and optical pH sensors monitor the concentrations of the protonated and deprotonated form of the indicator dye . The fiber-optic sensor scheme reported in this paper is different in its operation: it is based on determining the pH, through the change in the luminescence intensity. The Henderson-Hasselbalch equation is commonly used to determine the value of pH: changes of the deprotonated $[A^-]$ and protonated [HA] form are used, employing an optical signal method [22] where:

$$pH = pK_a - \log\frac{[HA]}{[A^-]} \quad (3)$$

Here pK_a is the acid-base constant of the indicator dye and $[A^-]$ and [HA] are related to fluorescence intensities observed, where $[A^-] = I_m - I_{min}$ and $[HA] = I_{max} - I_m$. I_m is the luminescence intensity monitored from the indicator and defining I_{max} as the maximum luminescence intensity signal of the deprotonated form (and I_{min} as the minimum

luminescence intensity signal of the protonated form), the pH in solution causing the change can be calculated by substituting these expressions into Eq. (3), and so:

$$pH = pK_a - b \cdot \log\left(\frac{I_{max} - I_m}{I_m - I_{min}}\right) \quad (4)$$

where b is the numerical coefficient.

3 Fabrication of fiber-optic probes and experimental set-up

A commercially available 400/430 µm (core/cladding) silica fiber was selected and this was purchased from Polymicro Technologies and used as the basis of the O_2 and pH probes. The key innovation was in the design of the fiber tip, which was specially formed using a thermal process to create a fiber diameter of < 50 µm. A commercial fusion splicer (Fujikura Arc Master FSM-100P+) was conveniently used to do this. The taper reduces the thickness of the cladding and thus increases the power fraction of the evanescent wave in the cladding to achieve a higher sensitivity to local changes of an applied coating [33]. The sensor tips were chemically treated to remove any remaining cladding – this was done to further increase the effective area over which the coating could be applied. The aim was to increase the sensitivity of the fiber tip and thereby optimize the light emission. In the final stage of probe construction, this specially tapered tip design was coated with an O_2 or pH-sensitive layer – the method to do this is now considered.

3.1 Preparation of the O_2 sensor probes

Chemicals used to prepare the O_2 sensitive coating were used as received from the manufacturers: PtTFPP (Frontier Scientific, Inc), PS (average Mw 2.500, Merck KGaA), chloroform (Merck KGaA) as well as toluene (Merck KGaA). These chemicals were of analytical grade with no further purification undertaken. An O_2-sensitve coating composition based on PtTFPP and polystyrene, comparable to that described [34], was prepared. A simple, fast dip-coating process was used where each pre-prepared fiber tip was first dipped into the O_2-sensitive coating composition and then, as shwn schematically in Figure 2 A and B, quickly removed. In that way it was possible to form the required thin PtTFPP-containing PS layers on the fiber-optic tips, having as a result the thin and reproducible coating that is needed for a practical sensor.

The coating thickness mainly depended on both the solution viscosity and the velocity of the tip withdrawal [35]. The process was optimized by experiment, in that way to create the conditions for a repeatable coating thicknesses taking advantage of this simple dip-coating approach. Although in this work this was done on a case-by-case basis by hand, it is capable of being scaled up and thus automated (a similar approach has been used in sensors designed for humidity monitoring and using a specially coated fiber optic [36, 37]). Each coated probe created was carefully dried at room temperature and under constant humidity (for 24 h), to allow any solvent remaining to dissipate. This then allowed the PtTFPP to be physically entrapped in the PS matrix, prior to the evaluation of the sensor performance in a systematic way, as discussed below.

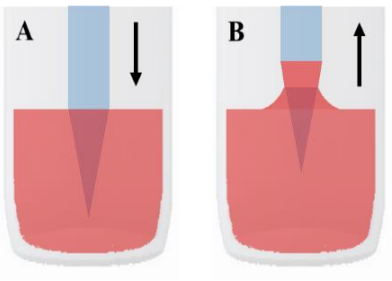

Fig 2. Schematic illustration of the dip-coating process. **A**: Fiber tip moved into coating mixture (red); **B**: Adhesion of coating material (red) when the fiber tip was extracted.

3.2 Preparation of the pH sensor probes

The fluorescent monomer used (fluorescein O-methacrylate) was well suited to the detection range pH 5.0 to pH 8.5, giving a strong luminescence signal. Fluorescein O-methacrylate is polymerizable, permitting covalent binding to be used – this is important as it can avoid the problem of dye leaching [38]. Further, the fluorescein is an indicator with the least negative charges (compared to other indicator dyes, such as HPTS) with a reduced dependence on ionic strength [39]. The work done thus took forward what has been reported in the literature [40], but importantly was enhanced to improve the coating process used.

A mixture of a number of chemicals was prepared: 2-hydroxyethyl methacrylate (HEMA), the photo-initiator 4-(2-hydroxyethoxy)phenyl-(2-hydroxy-2-propyl)ketone (Irgacure 2959) at 1.5%wt., 1,6-hexanediol diacrylate (HDDA) used at 5.0%wt. with respect to HEMA, the fluorescent monomer itself at 2.0%wt. with respect to HEMA and poly(ethylene glycol) diacrylate (PEGDA) at 3.0%wt. These were mixed fully using a magnetic stirrer and to allow photo-polymerization to occur, the fiber tip was dipped into the prepared mixture and light from a high power UV LED (365 nm peak wavelength, $P_0 \leq 500$mW) purchased from Omicron-Laserage GmbH was used to initiate the photopolymerization process – irradiating for a period of between 20 and 35 s, to form the thin, repeatable coatings needed on the fiber tip.

3.3 Experimental set-up and methods to characterize the O_2 probes

The experimental setup used to determine the performance of the O_2 sensors developed is shown in Figure 3, where the sensor probes were connected to a commercial instrument to allow the luminescence decay time to be monitored (this was supplied by neoFox from Ocean Insight Inc.). This set up was located in a closed chamber together with a reference O_2 sensing system (Microx TX3 and PSt1 sensor from PreSens Precision Sensing GmbH). The set up was temperature-regulated (over the range from 20°C to 80°C) with gas supplied via flow controllers to allow known quantities of O_2 (purity ≥ 99,999 %) and N_2 (purity ≥ 99,999 %) into the chamber. Different O_2 concentrations and temperatures could be generated fully automatically using a PC controller. In the work carried out, the luminescence decay times (in the µs range) were measured for each concentration of oxygen, from 0 % O_2 to 20 % O_2 (in steps of 4 % O_2) using the Lehrer quenching model (Eq. 3). The results obtained were compared with gas delivered using the regulated O_2 supply and the output of a conventional reference gas sensor. The set up allowed the probe response speed to be monitored – here a rapid change in the O_2 used (from 0 % to 20 % O_2 and back to 0 % O_2) was created in the chamber using the automated equipment.

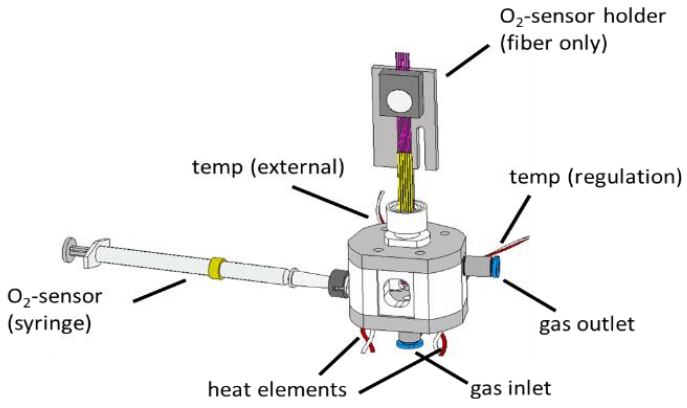

Fig 3. Illustration of the temperature regulated (20°C to 80°C) test chamber to generate stable O_2 concentrations for a range of 0 % O_2 – 100 % O_2. It allows the integration of O_2 sensors in a syringe housing and sensors without housing using the O_2 sensor holder. The valves connected to the input and output ports are not shown here.

Long-term drift of the probes could be analyzed (the 'photo-bleaching rate') using a solution containing 0 % O_2 prepared by adding 1 g sodium sulfite (Na_2SO_3) to 10 mL of distilled water, this being stirred until the Na_2SO_3 was completely dissolved. Then the bottle was closed with a silicone seal and the fiber-optic sensor inserted and

maintained for 12 h, while the luminescence decay time and intensity were monitored. In addition, the temperature was measured(in this case using a thermistor but a fiber optic sensor could easily be incorporated into the probe) in this case connected to the neoFox equipment. The sensor tip of the O_2 probe was continuously irradiated with light, at a pulse frequency of 4.85 kHz during this work.

In the next stage of the investigation, the tips of the fiber-optic sensors were placed in an ultrasonic cleaning bath filled with pure H_2O, the sensor was left there for 15 minutes and excited with green light from the neoFox instrument, in this way to evaluate mechanical stability and coating adhesion while a strong vibration signal was applied. Each sensor was individually calibrated and characterized before and after the experiment was carried out to investigate whether any damage occurs (e.g. detachment of the coating). The effect of temperature on the fiber-optic O_2 sensors was investigated (the physiological important range between 25°C and 40° was particularly investigated). Each sensor was investigated by being placed in the temperature-regulated chamber. The initial temperature was 25°C, following which concentrations of 0 %, 4 %, 8 %, 12 %, 16 % and 20 % O_2 were passed through the chamber for 30 s. This was repeated as temperature was increased in steps of 5°C, up to 40°C, and for each temperature and O_2 concentration, the luminescence decay time was monitored, averaging signals over 10 s time interval.

3.4 Experimental set-up and methods to characterize the pH probes

A newly designed instrument was used to characterize the pH sensors developed to monitor the weak luminescence emission signals from the pH-sensitive fiber tip coating and so to determine the pH value accurately. The instrument and sensor, that formed the system overall, can be seen in Figure 4. Here it was vital to reduce any effect of stray light, allowing it to work with very low excitation intensities – in that way allowing high quality long-term performance to be achieved, to maximize the sensor lifetime.

Each fiber-optic sensor was evaluated by connecting it to the optical port where the output was monitored by dipping it into each of five different pH buffers (at pH 5, pH 6, pH 7, pH 8 and pH 8.5) under stable temperature and pressure. The pH of the buffer solutions was checked each time before and after each measurement, using a reference pH electrode and ensuring temperature compensation of the fiber-optic sensing system (pH-1 micro and NTH-HP5 – purchased from PreSens Precision Sensing GmbH). This allowed the correction of the pH values by including calibration for temperature changes.

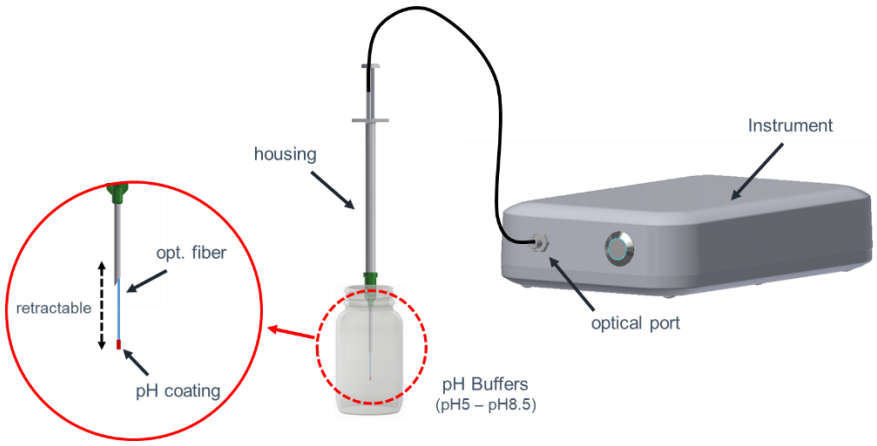

Fig 4. Experimental setup and the fiber-optic pH sensor design with the new sensor tip and the pH sensitive layer attached (red). The optical fiber is protected in a retractable housing.

During the system evaluation, the relative emission was first measured in each buffer solution (recorded in arbitrary units (a.u.)) and calibrated using Eq. 4. To carry out this, the pH sensors were inserted in a neutral solution (pH 7) and then quickly (< 1s) transferred to the pH 8 buffer solution to monitor the response time. Long-term sensor response drift was measured as the probe was maintained at pH 7 over a 12h period, during which the probe was irradiated continuously, to examine any photo-bleaching effects which may as a result occur.

The temperature stability of the pH buffer solutions was investigated using a temperature-compensated reference system (pH-1 micro and NTH-HP5). For this purpose, the temperature-induced pH changes of each buffer solution were investigated by comparing the measured pH values at 25°C and 40°C. To do so the temperature of the buffer solutions was raised in 5°C steps while being monitored with the use of a Pt100 sensor – the pH value was corrected using the reference system. At each temperature and pH value monitored, the relative sensor intensity was monitored, averaging the signals over ~3 minutes and the temperature-dependent sensor drift (arising from any photobleaching) was observed at pH7 and pH8 in buffer solutions, using different sampling intervals (on-off phase of the excitation light source) of 1 s (continuous irradiation) and 5 s (t_{on} = 1 sec t_{off} = 4 sec.).

4 Experimental results and discussion

These results below relate to the fiber-optic O_2 and pH probes fabricated, using the experimental set-ups described above. Key parameters considered here include system calibration, accuracy, response time, long-term and mechanical stability as well as cross-sensitivities to temperature. The following sections discuss the outcomes of these investigations.

4.1 Calibration results and response times of the fiber-optic O_2 and pH probes

Both sensor probes developed show a change in the luminescence signal induced by the 'analyte', giving a decay time change for the O_2 probe and a change in intensity for the pH probe. Each sensor was calibrated as discussed above, with the results obtained illustrated in Figure 5. The dashed lines represent the data fitted to the Lehrer model (for the O_2 probe) and the Henderson-Hasselbalch equation, when using a pH-sensitive fiber tip coating. Both models clearly describe experimental results with a high level of precision – for the O_2 sensor probe, the correlation coefficient has a very high value of R^2 (= 0.9999), allowing very accurate measurements of O_2. The sensors represent the highest sensitivity for low O_2 concentrations due to the maximum dynamic range between 0 % and 4 % O_2, achieving a very good response for the measurement overall.

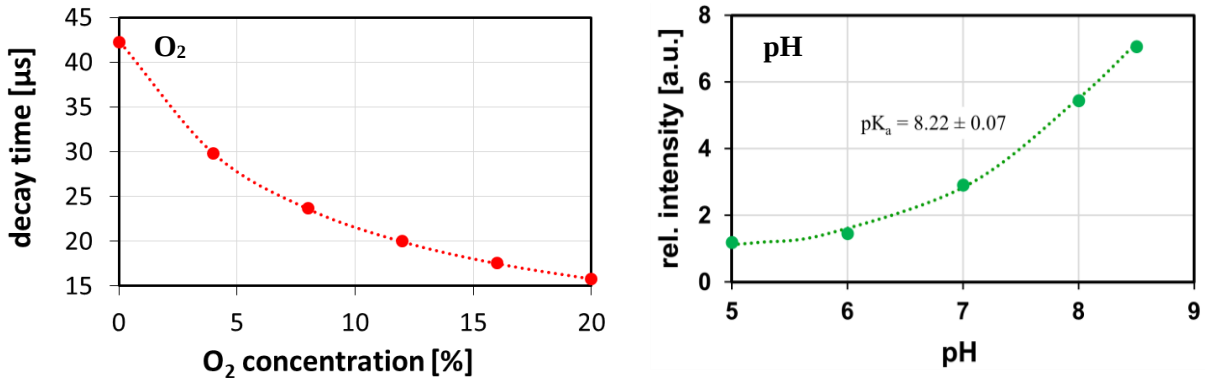

Fig 5. Calibration curves of a fiber-optic O_2 (**red**) and pH probe (**green**) with the specially tapered tip. Each data point determined at steady state and averaged over the range of 50 s (50 sampling points). The dashed red curve represents the fitted Lehrer model applying Eq. 2 and the dashed curve the fitted Henderson-Hasselbalch applying equation Eq. 4.

The correlation coefficient (R^2 = 0.9991) of the pH probe determined in this work is slightly lower than could have been expected, but the sensor accuracy is approximately ±0.04 pH units (at pH 7) – this is very well suited to many measurement situations. Experimentally, pK_a was determined to have a value of 8.22 ± 0.07 – this is slightly higher than was reported for a comparable sensing film (pK_a = 7.9) [40]. It is known that the pK_a value of luminescent indicators changes with the environment [41] and can shift to a higher value by changing the polarity of the microenvironment (e.g. when using different polymers) [42].

Figure 6 shows the performance of a calibrated O_2 (red) and pH (green) sensor probe, revealing the rapid response seen from both sensor designs and an average sensor accuracy in the detection of O_2 concentration (red) of better than ±0.03 % O_2 across the overall detection range. The system calibration was done by using the measured volume flows of the thermal mass flow meters/controllers for N_2 and O_2 as a reference. The changes in pH (shown in green) have been measured from pH 5 to pH 8.5 with a maximum signal variation (equivalent to < 0.01 pH units) and obtained for pH values greater than pH 6. It is important to note than an excellent signal-to-noise ratio is evident from the data obtained, in spite of the very thin coatings used.

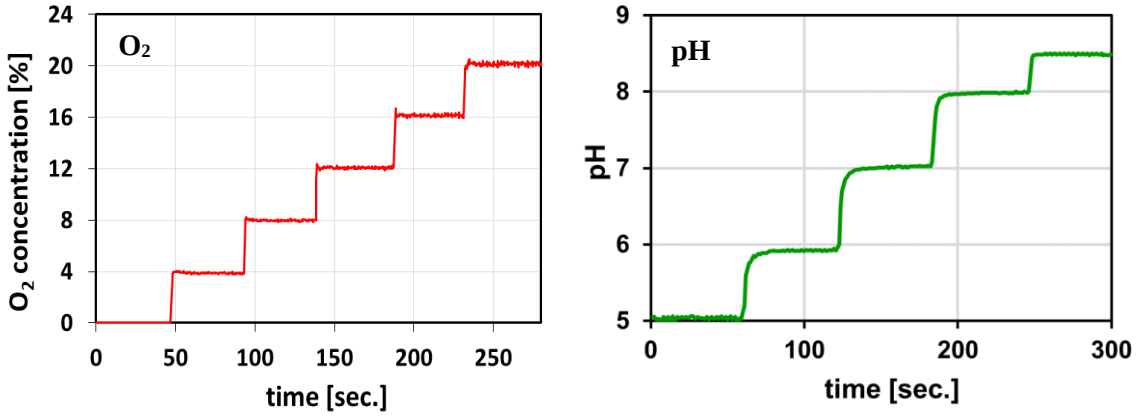

Fig 6. Measured O_2 changes of a calibrated O_2 probe in gaseous O_2 (**red**) and measured pH changes of a calibrated pH probe in pH buffer solutions (**green**). Both measurements were performed at a constant temperature of 25°C and also illustrate the rapid response of the probes.

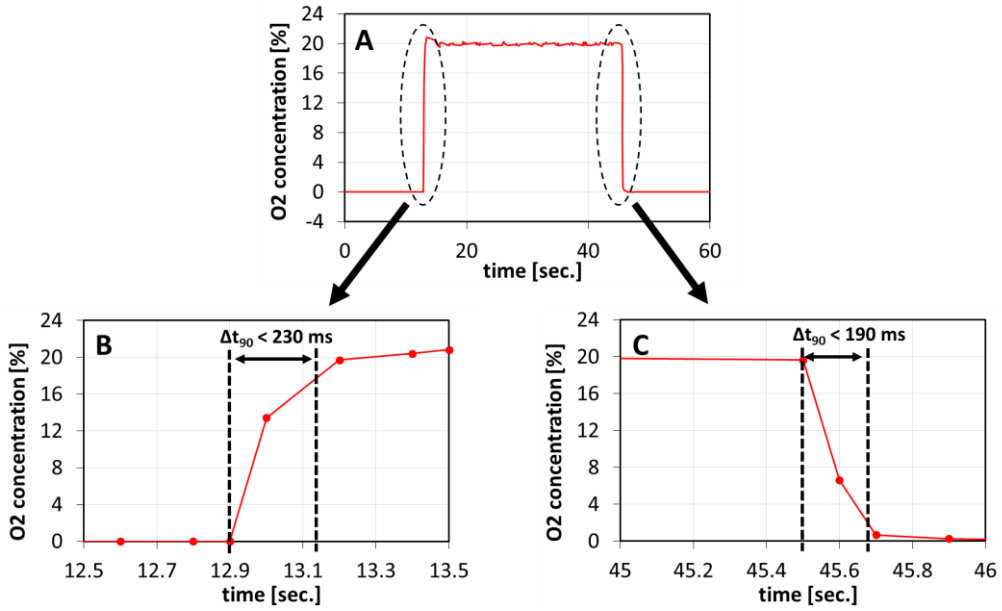

Fig 7. Measured response time of the O_2 probe due to a rapid change from 0 % to 20 % O_2 and back to 0 % O_2 again (**A**). (**B**) shows the rise time of the probe ($\Delta t_{90} \approx 230$ ms) and (**C**) the fall time of the probe ($\Delta t_{90} \approx 190$ ms).

The response time of the O_2 sensor design has been studied in some detail (as shown in Figure 7) and the rapid response that has been an important feature of the design is seen over the detection range from 0 % to 20 % O_2, (and back to 0 % O_2 again). An overall response time of $\Delta t_{90} \approx 230$ ms for *increasing* O_2 concentrations, and an even faster response time of $\Delta t_{90min} \approx 190$ ms for *decreasing* O_2 concentrations has been seen. The narrow profile

tip design is the key feature which enables this fast response to be obtained, coupled to the very thin coatings, while still allowing the detection of luminescence signals over a large effective tip area, with a much faster diffusion of O_2. Further tests show that the probes have a comparable, rapid response to O_2 changes over the range studied, as shown in Figure 6. In addition, the performance compares very well with published data from other optical sensor designs using comparable PtTFPP- or PtOEP-containing coatings. Typically such sensor designs have response times of between 3.7 s and 100 s [26–30], which is much greater than for the probe designed here and reported in this work.

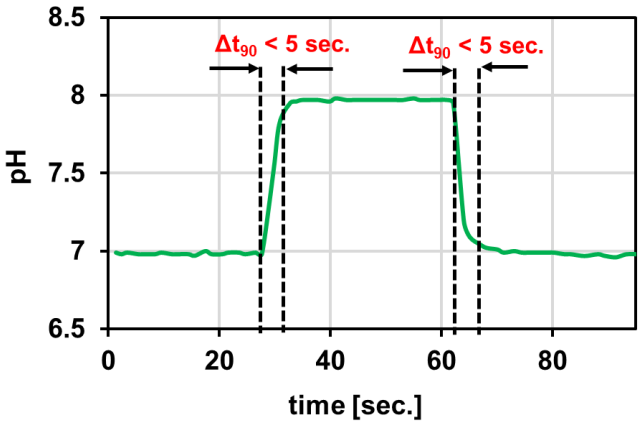

Fig 8. Measured response time of the pH probe due to a due to a rapid transfer (~1 s) from pH 7 to pH 8 and back to pH 7 again showing a rise and fall time of < 5 s.

Figure 8 shows data on the response time where it has been shown to have a very fast response to pH changes, of Δt_{90} < 5s (with the period of ~1s taken to move the sensor physically from one buffer solution to another also included). This has been studied over pH 7 to pH 8, and back to pH7 and again when compared to the data published on a wide range of pH sensors in the literature shows a major advantage. The response time depends on the initial and final pH value, as shown in Figure 6: for pH values below pH 7 the response time was slightly slower, however, this was faster for pH values > pH 8.

4.2 Long-term stability (photostability) of the probe designs

Figure 9 shows the results of longer-term measurements made with the O_2 and pH sensor probe for an extended period of 12 h. For this purpose, the probes were continuously irradiated with the light of the instruments used to investigate the drift of the luminescence decay time (for O_2) or the luminescence intensity (for pH) resulting from photobleaching. The O_2 probe was placed in a stable 0 % O_2 solution and the pH probe was placed in stable buffer solution of pH 7, with each measurement taken in an almost temperature-stable environment of 25°C. Temperature was seen to be very stable ($\Delta T_{max} \approx 0.46$°C) over all the experiments carried out.

The pH sensor probe was seen to be very stable when compared to what has been reported (drift being < 2.42 %/h), even though the pH monitoring was based on luminescence intensity monitoring. For this worst-case scenario (continuous irradiation and a sampling rate of 1 s) assuming that a sensor drift error of < 0.05 pH/h was acceptable, a re-calibration of the sensor would only be required after 3600 data points.

Looking at the O_2 sensor probe, the drift observed of ~0.007 %/h was extremely low. A further positive feature of the probe was that the luminescence decay time measurement was significantly less affected by either photobleaching or light source instability (drift), as well as photodetector sensitivity. However, even with continuous irradiation and a sampling rate of 0.5 s, the sensors show an exceptional long-term stability. This means that the probe does not need regular recalibration. When a measurement error of ≈ 0.5 % O_2 (for O_2 concentrations < 20 % O_2) is allowed, the sensor would only need a re-calibration after 144000 data points or 20 h of continuous measurement (with a sampling rate of 0.5 s). This is much longer than is needed for many biomedical applications.

Higher sensitivity of the sensor at very low O_2 concentrations (< 4 %O_2) is seen and here a re-calibration after a longer period of 890000 data points (or a measurement duration of 124 h) is appropriate to this O_2 measurement region.

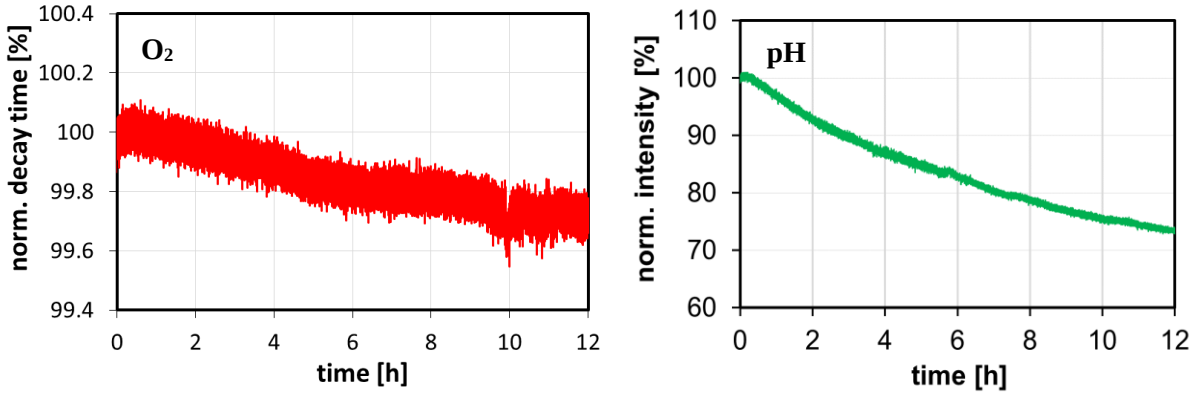

Fig 9. Long-term drift of an O_2 (**red**) and pH probe (**green**) seen under continuous irradiation for 12 h. **Red:** decrease of luminescence decay time of an O_2 probe when placed in a stable 0 % O_2 solution; **Green**: Luminescence signal decrease of a pH probe when placed in a stable buffer solution of pH 7. A constant temperature of 25°C was used.

4.3 Effect of temperature on the probe designs

Temperature drift effects are likely to be the biggest source of error in optical luminescence-based sensors [21], and so the effect of temperature on both sensor designs (O_2 and pH) has been studied over 25°C and 40°C (in steps of 5°C) using the setups and procedures described.

The results obtained for the O_2 sensor probe showed the expected effect on the luminescence lifetime, as it shortens the luminescence lifetimes of PtTFPP for increasing temperature (and this has been used very effectively in stand-alone temperature sensors [43]). As expected, the obtained calibration curves show a general shift to lower decay times for increasing temperature values and thus an increase in the absolute O_2 error for higher O_2 concentrations. This temperature-induced signal drift shows a linear behavior over the O_2 range between 0% and 20% O_2 and is shown in Figure 10 (left). However, temperature compensation can readily be incorporated in the probe. A technique that can be applied is using a small length of rare-earth doped fiber whose decay time will also change with temperature, but is unaffected by O_2 concentration changes [44], or to include a Fiber Bragg Grating or a Long Period Grating temperature sensor [45].

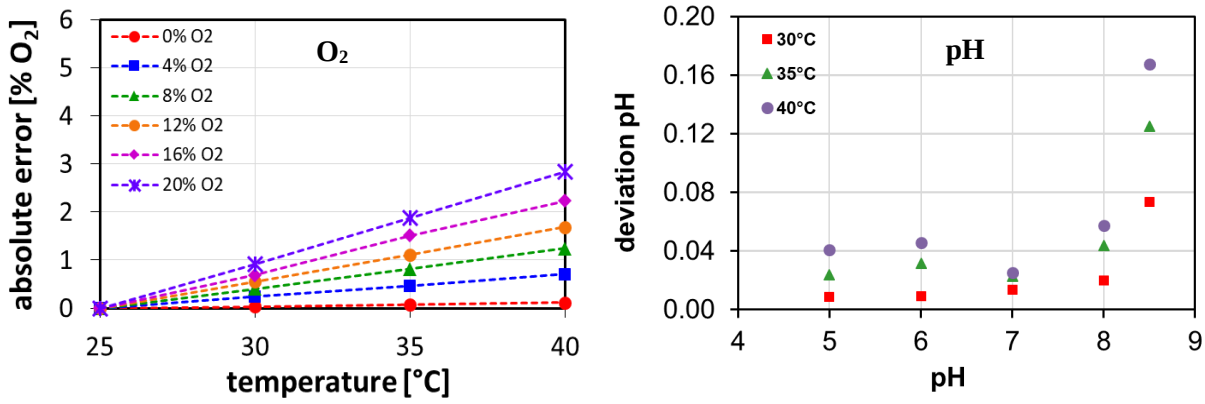

Fig 10. Effect of temperature on the O_2 (**left**) and pH sensor (**right**) designs. **Left**: shows the absolute O_2 error (% O_2) over temperature (between 25°C and 40°C) and determined for O_2 concentrations between 0 % and 20 % O_2. **Right**: shows the temperature induced deviation of pH compared to the reference values at a temperature of 25°C.

In contrast to the O_2 probe, the pH sensor unexpectedly showed no significant influence to temperature changes for pH values below pH 8 and the temperature range investigated. To illustrate these minor changes, Figure 10 (right) shows the change in the pH value over the entire detection range between pH 5 and pH 8.5 and at temperature values of 30°C, 35°C and 40°C, when compared to the "reference values" determined at 25°C. However, temperature exerts somewhat complex effects on pH-sensitive materials and influences other parameters such as the swelling ratio of the hydrogel [46], and in the case of the luminescence-based sensor, the thermal quenching of the luminescence of the pH indicator [47]. Further work shows that the decrease of luminescence emissions for pH values ≥ pH 8 seems mainly to be influenced by a higher bleaching rate of the indicator at higher temperatures [48].

4.4 Mechanical stability of the probe designs

Good mechanical stability for many industrial uses is important, and Figure 11 show results when an O_2 and a pH probe experienced strong vibrations, when using the procedures described in the previous section. Figure 11 (left) shows the calibration curves of an O_2 probe before and after exposure to vibrations and Figure 11 (right) shows continuous measurement data of a pH probe in pH 6, pH 7 and pH 8.

Both coatings show really good performance –strong adhesion to the fiber tip surface is seen and no mechanical damage is observed when the tip was examined under a microscope. No significant signal changes have been measured, when comparing the calibration curves of the O_2 probe, and no detachment of the coating occurred during the experiments carried out. Only at pH 8 does the signal decrease after the ultrasonic cleaner is turned on – explained by the higher bleaching rate of the indicator, at higher temperatures, generated by a temperature change from 25°C to 38°C from the ultrasonic sample irradiation – so the probes can be used in harsh environments where these are mechanically stressed without the need of a re-calibration.

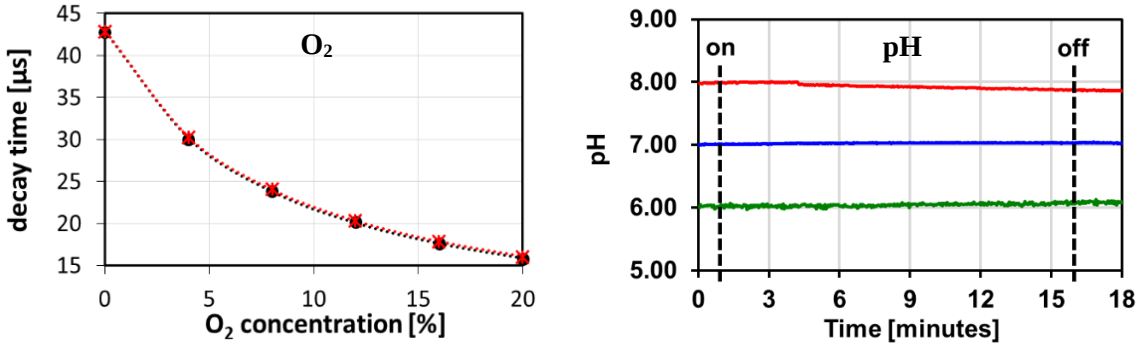

Fig 11. Mechanical stability of the O_2 (**left**) and pH sensor (**right**) designs. **Left**: Measured calibration curves of a O_2 probe in gaseous O_2 before (black) and after (red) the sensor was hold in an ultrasonic cleaner for 15 minutes. **Right**: Continuously measured pH values of a pH probe in pH 6 (green), pH 7 (blue) and pH 8 (red) solutions and under strong vibrations. An ultrasonic cleaner provided the vibration effect, by being turned on after 1 minute and off after 16 minutes (black, dashed).

5 Conclusions

This work has discussed a range of new fiber optic pH and O_2 sensing systems which have been developed and evaluated. These have been based on new probe tip designs and the use of luminescence-based coatings. Highly promising results have been obtained, showing significant improvement of the sensor performance on current devices. Importantly, extremely fast response times to O_2 ($\Delta t_{90} < 400$ ms) and pH ($\Delta t_{90} < 5$ s) changes have been reported. The unique characteristics seen have resulted from an increased effective area of what was still a very compact sensor tip, allowing an optimization of the light emission from the probe. In this way, it has permitted the use of thinner coatings on the fiber tip itself without compromising the signal-to-noise ratio.

Thus highly accurate measurements of pH and O_2 have been shown possible using very small sample volumes, because of the design with small optical fibers and small fiber tip diameters. The work has prioritized monitoring of small volume samples, which often all that is available from biological or clinical work. In combination with newly developed instrumentation, the pH sensors have been shown to be very stable over a long period of time, as during a measurement for 12 hours at pH 7 with continuous irradiation, a low signal drift (of less than 0.05 pH/h) and a negligible influence of stray light were observed.

The O_2 probe showed an exceptional long-term stability, only a drift of $\Delta\tau_{max} \approx 0.007$ %/h seen in a comparable 12 h experiment. A potential user would therefore only need to re-calibrate the sensors after a long period of time, which is ideal for widespread use of such sensors. Furthermore, the temperature 'crosstalk', which can be a problem with many such sensor designs, was investigated in the physiologically relevant temperature range (between 25°C and 40°C). Excellent temperature stability of the sensor design itself was seen, while a relative simple temperature compensation is suggested by incorporating a further fiber-optic based temperature sensor in the probe.

The work has clearly showed that this new sensor design has the potential to extend the breadth of applications for fiber-optic pH and O_2 sensors, especially where fast response times are required. A further benefit of this design for biological or clinical applications is that the manufacturing process for these sensors is relatively simple and thus volume production, at low cost, is feasible – creating an approach which will also suit a range of applications including those where easy and inexpensive disposal of the sensor probe is required after each use.

Acknowledgemets

The authors wish to acknowledge Alexander Schäfer for the great support in software development and would like to thank WPI GmbH for the financial support. Grattan and Sun acknowledge support from the Royal Academy of Engineering.

References

[1] S. Kojima and H. Suzuki, "A Micro Sensing System for Blood Gas Analysis Constructed With Stacked Modules," *IEEJ Trans. SM*, vol. 124, no. 4, pp. 111–116, 2004, doi: 10.1541/ieejsmas.124.111.

[2] D. B. Papkovsky, N. Papkovskaia, A. Smyth, J. Kerry, and V. I. Ogurtsov, "Phosphorescent Sensor Approach for Non-Destructive Measurement of Oxygen in Packaged Foods: Optimisation of Disposable Oxygen Sensors and their Characterization Over a Wide Temperature Range," *Analytical Letters*, vol. 33, no. 9, pp. 1755–1777, 2000, doi: 10.1080/00032710008543157.

[3] A. S. Jeevarajan, S. Vani, T. D. Taylor, and M. M. Anderson, "Continuous pH monitoring in a perfused bioreactor system using an optical pH sensor," *Biotechnology and bioengineering*, vol. 78, no. 4, pp. 467–472, 2002, doi: 10.1002/bit.10212.

[4] Y. Kostov, P. Harms, L. Randers-Eichhorn, and G. Rao, "Low-cost microbioreactor for high-throughput bioprocessing," *Biotechnol. Bioeng.*, vol. 72, no. 3, pp. 346–352, 2001, doi: 10.1002/1097-0290(20010205)72:3<346::aid-bit12>3.0.co;2-x.

[5] J. F. Gouin, F. Baros, D. Birot, and J. C. André, "A fibre-optic oxygen sensor for oceanography," *Sensors and Actuators B: Chemical*, vol. 39, 1-3, pp. 401–406, 1997, doi: 10.1016/S0925-4005(97)80242-0.

[6] C. R. Schröder, B. M. Weidgans, and I. Klimant, "pH fluorosensors for use in marine systems," *The Analyst*, vol. 130, no. 6, pp. 907–916, 2005, doi: 10.1039/B501306B.

[7] J. Werner, M. Belz, K.-F. Klein, T. Sun, and K.T.V. Grattan, "Fiber optic sensor designs and luminescence-based methods for the detection of oxygen and pH measurement," *Measurement*, vol. 178, p. 109323, 2021, doi: 10.1016/j.measurement.2021.109323.

[8] L. C. CLARK, R. WOLF, D. GRANGER, and Z. TAYLOR, "Continuous recording of blood oxygen tensions by polarography," *Journal of applied physiology*, vol. 6, no. 3, pp. 189–193, 1953, doi: 10.1152/jappl.1953.6.3.189.

[9] P. T. Kerridge, “The Use of the Glass Electrode in Biochemistry,” *The Biochemical journal*, vol. 19, no. 4, pp. 611–617, 1925, doi: 10.1042/bj0190611.
[10] X.-d. Wang and O. S. Wolfbeis, “Fiber-optic chemical sensors and biosensors (2008-2012),” *Analytical chemistry*, vol. 85, no. 2, pp. 487–508, 2013, doi: 10.1021/ac303159b.
[11] C. Staudinger *et al.*, “A versatile optode system for oxygen, carbon dioxide, and pH measurements in seawater with integrated battery and logger,” *Limnol. Oceanogr. Methods*, vol. 16, no. 7, pp. 459–473, 2018, doi: 10.1002/lom3.10260.
[12] C. G. Frankær, K. J. Hussain, T. C. Dörge, and T. J. Sørensen, “Optical Chemical Sensor Using Intensity Ratiometric Fluorescence Signals for Fast and Reliable pH Determination,” *ACS sensors*, vol. 4, no. 1, pp. 26–31, 2019, doi: 10.1021/acssensors.8b01485.
[13] PyroScience GmbH, *AquapHOx: Underwater Oxygen Sensors*. Datasheet. [Online]. Available: https://www.pyroscience.com/en/applications/applications/underwater-solution (accessed: Nov. 24 2020).
[14] PyroScience GmbH, *PHROBSC-PK6: Robust pH Screw Cap Probe*. Datasheet. [Online]. Available: https://www.pyroscience.com/en/products/all-sensors/phrobsc-pk6#Downloads (accessed: Nov. 24 2020).
[15] D. Wencel *et al.*, “Optical Sensor for Real-Time pH Monitoring in Human Tissue,” *Small (Weinheim an der Bergstrasse, Germany)*, vol. 14, no. 51, e1803627, 2018, doi: 10.1002/smll.201803627.
[16] S. Chen, Q. Yang, H. Xiao, H. Shi, and Y. Ma, “Local pH Monitoring of Small Cluster of Cells using a Fiber-Optic Dual-Core Micro-Probe,” *Sensors and Actuators B: Chemical*, vol. 241, pp. 398–405, 2017, doi: 10.1016/j.snb.2016.10.079.
[17] Q. Yang *et al.*, “Fiber-Optic-Based Micro-Probe Using Hexagonal 1-in-6 Fiber Configuration for Intracellular Single-Cell pH Measurement,” *Analytical chemistry*, vol. 87, no. 14, pp. 7171–7179, 2015, doi: 10.1021/acs.analchem.5b01040.
[18] PreSens Precision Sensing GmbH, *PM-HP5: pH Microsensor*. [Online]. Available: https://www.presens.de/products/detail/profiling-ph-microsensor-pm-hp5 (accessed: Nov. 24 2020).
[19] U. Kosch, I. Klimant, and O. S. Wolfbeis, “Long-lifetime based pH micro-optodes without oxygen interference,” *Fresenius' Journal of Analytical Chemistry*, vol. 364, 1-2, pp. 48–53, 1999, doi: 10.1007/s002160051299.
[20] D. Wencel, B. D. MacCraith, and C. McDonagh, “High performance optical ratiometric sol–gel-based pH sensor,” *Sensors and Actuators B: Chemical*, vol. 139, no. 1, pp. 208–213, 2009, doi: 10.1016/j.snb.2008.12.066.
[21] X.-d. Wang and O. S. Wolfbeis, “Optical methods for sensing and imaging oxygen: materials, spectroscopies and applications,” *Chemical Society reviews*, vol. 43, no. 10, pp. 3666–3761, 2014, doi: 10.1039/C4CS00039K.
[22] D. Wencel, T. Abel, and C. McDonagh, “Optical chemical pH sensors,” *Analytical chemistry*, vol. 86, no. 1, pp. 15–29, 2014, doi: 10.1021/ac4035168.
[23] C. McDonagh, C. S. Burke, and B. D. MacCraith, “Optical chemical sensors,” *Chemical reviews*, vol. 108, no. 2, pp. 400–422, 2008, doi: 10.1021/cr068102g.
[24] K.-F. Klein, C.P. Gonschior, X.Ruan, M.Bloos, G.Hillrichs, H.Poisel, “Transmission of skew modes in polymer- and silica-based step-index fibers,” *Proc. 18th POF-conference*, no. 45, 2009.
[25] Arne Wilhelm Zimmer, Philipp Raithel, Mathias Belz, Karl-Friedrich Klein, “Analysis of spectral light guidance in specialty fibers,” *in Proc. SPIE 9886-34*, 2016.
[26] C.-S. Chu and Y.-L. Lo, “High-performance fiber-optic oxygen sensors based on fluorinated xerogels doped with Pt(II) complexes,” *Sensors and Actuators B: Chemical*, vol. 124, no. 2, pp. 376–382, 2007, doi: 10.1016/j.snb.2006.12.049.
[27] G. Holst, R. N. Glud, M. Kühl, and I. Klimant, “A microoptode array for fine-scale measurement of oxygen distribution,” *Sensors and Actuators B: Chemical*, vol. 38, 1-3, pp. 122–129, 1997, doi: 10.1016/S0925-4005(97)80181-5.
[28] S.-K. Lee and I. Okura, “Optical Sensor for Oxygen Using a Porphyrin-doped Sol–Gel Glass,” *Analyst*, vol. 122, no. 1, pp. 81–84, 1997, doi: 10.1039/A604885D.

[29] S.-K. Lee and I. Okura, “Photoluminescent determination of oxygen using metalloporphyrin-polymer sensing systems,” *Spectrochimica Acta Part A: Molecular and Biomolecular Spectroscopy*, vol. 54, no. 1, pp. 91–100, 1998, doi: 10.1016/S1386-1425(97)00206-0.
[30] G. R. McDowell, A. S. Holmes-Smith, M. Uttamlal, C. Mitchell, and P. H. Shannon, “A robust and reliable optical trace oxygen sensor,” *SPIE, Optical Sensors*, Vol. 10231, 2017, doi: 10.1117/12.2265561.
[31] T. H. Nguyen *et al.*, “Fluorescence based fibre optic pH sensor for the pH 10–13 range suitable for corrosion monitoring in concrete structures,” *Sensors and Actuators B: Chemical*, vol. 191, pp. 498–507, 2014, doi: 10.1016/j.snb.2013.09.072.
[32] J. R. Lakowicz, Ed., *Principles of Fluorescence Spectroscopy*. Boston, MA: Springer US, 2006.
[33] S. Guo and S. Albin, “Transmission property and evanescent wave absorption of cladded multimode fiber tapers,” *Optics express*, vol. 11, no. 3, pp. 215–223, 2003, doi: 10.1364/OE.11.000215.
[34] S.-K. Lee and I. Okura, “Photostable Optical Oxygen Sensing Material: Platinum Tetrakis(pentafluorophenyl)porphyrin Immobilized in Polystyrene,” *Anal. Commun.*, vol. 34, no. 6, pp. 185–188, 1997, doi: 10.1039/A701130J.
[35] D. Quéré, “FLUID COATING ON A FIBER,” *Annu. Rev. Fluid Mech.*, vol. 31, no. 1, pp. 347–384, 1999, doi: 10.1146/annurev.fluid.31.1.347.
[36] L. Alwis, K. Bremer, T. Sun, and K. T. V. Grattan, “Analysis of the Characteristics of PVA-Coated LPG-Based Sensors to Coating Thickness and Changes in the External Refractive Index,” *IEEE Sensors J.*, vol. 13, no. 3, pp. 1117–1124, 2013, doi: 10.1109/JSEN.2012.2230534.
[37] B. Rente *et al.*, “Extended Study of Fiber Optic-Based Humidity Sensing System Performance for Sewer Network Condition Monitoring,” *IEEE Sensors J.*, vol. 21, no. 6, pp. 7665–7671, 2021, doi: 10.1109/JSEN.2021.3050341.
[38] A. M. Breul, M. D. Hager, and U. S. Schubert, “Fluorescent monomers as building blocks for dye labeled polymers: synthesis and application in energy conversion, biolabeling and sensors,” *Chemical Society reviews*, vol. 42, no. 12, pp. 5366–5407, 2013, doi: 10.1039/C3CS35478D.
[39] B. M. Weidgans, “New fluorescent optical pH sensors with minimal effects of ionic strength,” Universität Regensburg, 2004.
[40] L. Rovati, S. Cattini, P. Fabbri, and L. Ferrari, “Fluorescence pH Sensor Based on Polymer Film,” in *2018 International Flexible Electronics Technology Conference (IFETC)*, Ottawa, ON, Aug. 2018 - Aug. 2018, pp. 1–5.
[41] L. D. Lavis, T. J. Rutkoski, and R. T. Raines, “Tuning the pK(a) of fluorescein to optimize binding assays,” *Anal. Chem.*, vol. 79, no. 17, pp. 6775–6782, 2007, doi: 10.1021/ac070907g.
[42] A. S. Vasylevska, A. A. Karasyov, S. M. Borisov, and C. Krause, “Novel coumarin-based fluorescent pH indicators, probes and membranes covering a broad pH range,” *Analytical and bioanalytical chemistry*, vol. 387, no. 6, pp. 2131–2141, 2007, doi: 10.1007/s00216-006-1061-6.
[43] T. Sun, Z. Y. Zhang, K. T. V. Grattan, and A. W. Palmer, “Ytterbium-based fluorescence decay time fiber optic temperature sensor systems,” *Review of Scientific Instruments*, vol. 69, no. 12, pp. 4179–4185, 1998, doi: 10.1063/1.1149267.
[44] T. Sun, Z. Y. Zhang, and K. T. V. Grattan, “Erbium/ytterbium fluorescence based fiber optic temperature sensor system,” *Rev. Sci. Instrum.*, vol. 71, no. 11, p. 4017, 2000, doi: 10.1063/1.1289682.
[45] S. K. Abi Kaed Bey, T. Sun, and K. T.V. Grattan, “Sensitivity enhancement of long period gratings for temperature measurement using the long period grating pair technique,” *Sensors and Actuators A: Physical*, vol. 141, no. 2, pp. 314–320, 2008, doi: 10.1016/j.sna.2007.10.019.
[46] H. van der Linden and J. Westerweel, “Temperature-Sensitive Hydrogels,” in *Encyclopedia of Microfluidics and Nanofluidics*, D. Li, Ed., Boston, MA: Springer US, 2013, pp. 1–5.
[47] A. Steinegger, O. S. Wolfbeis, and S. M. Borisov, “Optical Sensing and Imaging of pH Values: Spectroscopies, Materials, and Applications,” *Chemical reviews*, vol. 120, no. 22, pp. 12357–12489, 2020, doi: 10.1021/acs.chemrev.0c00451.

[48] J. Werner, M. Belz, K.-F. Klein, T. Sun, and K. T. V. Grattan, “Characterization of a fast response fiber-optic pH sensor and illustration in a biological application,” *Analyst*, vol. 146, no. 15, pp. 4811–4821, 2021, doi: 10.1039/D1AN00631B.

_____

Corresponding author

e mail: jan.werner@city.ac.uk (Jan Werner)